

The Taurus Molecular Cloud: Multi-Wavelength Surveys with XMM-Newton, the Spitzer Space Telescope, and CFHT¹

Manuel Güdel

Paul Scherrer Institut

Deborah L. Padgett

California Institute of Technology

Catherine Dougados

Laboratoire d'Astrophysique de Grenoble

The Taurus Molecular Cloud (TMC) ranks among the nearest and best-studied low-mass star formation regions. It contains numerous prototypical examples of deeply embedded protostars with massive disks and outflows, classical and weak-lined T Tauri stars, jets and Herbig-Haro objects, and a growing number of confirmed brown dwarfs. Star formation is ongoing, and the cloud covers all stages of pre-main sequence stellar evolution. We have initiated comprehensive surveys of the TMC, in particular including: (i) a deep X-ray survey of about 5 sq. degrees with *XMM-Newton*; (ii) a near-to-mid-infrared photometric survey of ≈ 30 sq. degrees with the Spitzer Space Telescope, mapping the entire cloud in all available photometric bands; and (iii) a deep optical survey using the Canada-France-Hawaii Telescope. Each wavelength regime contributes to the understanding of different aspects of young stellar systems. *XMM-Newton* and Spitzer mapping of the central TMC is a real breakthrough in disk characterization, offering the most detailed studies of correlations between disk properties and high-energy magnetic processes in any low-mass star-forming region, extending also to brown dwarfs in which disk physics is largely unexplored. The optical data critically complements the other two surveys by allowing clear source identification with $0.8''$ resolution, identifying substellar candidates, and, when combined with NIR data, providing the wavelength baseline to probe NIR excess emission. We report results and correlation studies from these surveys. In particular, we address the physical interpretation of our new X-ray data, discuss the entire young stellar population from embedded protostars to weak-lined T Tau stars and their environment, and present new results on the low-mass population of the TMC, including young brown dwarfs.

1. INTRODUCTION

In a modern picture of star formation, complex feedback loops regulate mass accretion processes, the ejection of jets and outflows, and the chemical and physical evolution of disk material destined to form planets. Observations in X-rays with *Chandra* and *XMM-Newton* penetrate dense molecular envelopes, revealing an environment exposed to high levels of X-ray radiation. In a complementary manner, observations in the infrared with the *Spitzer Space Telescope* (*Spitzer*) now obtain detailed infrared photometry and spectroscopy with diagnostics for disk structure and chemical composition of the gas and dust in the circumstel-

lar environment. Furthermore, optical surveys have reached a sensitivity and area coverage with which a detailed census of the substellar population has become possible.

Near- to far-infrared (IR) emission originates predominantly in the dusty environment of the forming stars, either in contracting gaseous envelopes or in circumstellar disks. IR excess (relative to the photospheric contributions) has been successfully used to model disk geometry, the structure of the envelope, and also the composition and structure of dust grains (*d'Alessio et al.*, 1999).

X-rays play a crucial role in studies of star formation, both physically and diagnostically. They may be generated at various locations in young stellar systems, such as in a “solar-like” coronal/magnetospheric environment, in shocks forming in accretion funnel flows (e.g., *Kastner et al.*, 2002), or in jets and Herbig-Haro flows (e.g., *Pravdo et al.*, 2001; *Bally et al.*, 2003; *Güdel et al.*, 2005). By ionizing circumstellar material, X-rays also determine some of the prevalent chemistry (*Glassgold et al.*, 2004) while making the gas accessible to magnetic fields. Ionization of the

¹With significant contributions from: Lori Allen (CfA), Marc Audard (Columbia University), Jérôme Bouvier (Grenoble), Kevin Briggs (PSI), Sean Carey (Caltech), Elena Franciosini (Palermo), Misato Fukagawa (Caltech), Nicolas Grosso (Grenoble), Sylvain Guieu (Grenoble), Dean Hines (Space Science Institute), Tracy Huard (CfA), Eugene Magnier (IfA Honolulu), Eduardo Martín (IAC, Spain), François Ménard (Grenoble), Jean-Louis Monin (Grenoble), Alberto Noriega-Crespo (Caltech), Francesco Palla (Florence), Luisa Rebull (Caltech), Luigi Scelsi (Palermo), Alessandra Telleschi (PSI), Susan Terebey (CalStateLA).

circumstellar-disk surface may further drive accretion instabilities (*Balbus and Hawley, 1991*). Many of these X-ray related issues are summarized in the chapter by *Feigelson et al.* in this volume, based on recent X-ray observations of star-forming regions.

1.1 The Taurus Molecular Cloud Complex

The Taurus Molecular Cloud (TMC henceforth) has played a fundamental role in our understanding of low-mass star formation. At a distance around 140 pc (e.g., *Loinard et al., 2005; Kenyon et al., 1994*), it is one of the nearest star formation regions (SFR) and reveals characteristics that make it ideal for detailed physical studies. One of the most notable properties of the TMC in this regard is its structure in which several loosely associated but otherwise rather isolated molecular cores each produce one or only a few low-mass stars, different from the much denser cores in ρ Oph or in Orion. TMC features a low stellar density of only 1–10 stars pc⁻² (e.g., *Gómez et al., 1993*). Strong mutual influence due to outflows, jets, or gravitational effects are therefore minimized. Further, most stars in TMC are subject to relatively modest extinction, providing access to a broad spectrum of stars at all evolutionary stages from Class 0 sources to near-zero age main-sequence T Tau stars. TMC has also become of central interest for the study of substellar objects, in particular brown dwarfs (BD), with regard to their evolutionary history and their spatial distribution and dispersal (*Reipurth and Clarke, 2001; Briceño et al., 2002*).

TMC has figured prominently in star-formation studies at all wavelengths. It has provided the best-characterized sample of classical and weak-lined T Tau stars (CTTS and WTTS, respectively, or “Class II” and “Class III” objects - *Kenyon and Hartmann, 1995*); most of our current picture of low-density star formation is indeed based on IRAS studies of TMC (*Beichman et al., 1986; Myers et al., 1987; Strom et al., 1989; Kenyon et al., 1990; Weaver and Jones, 1992; and Kenyon and Hartmann, 1995*). Among the key results from TMC studies as listed in *Kenyon and Hartmann (1995)* figure the following: i) More than 50% of the TMC objects have IR excess beyond the photospheric contribution, correlating with other activity indicators ($H\alpha$, UV excess etc.) and indicating the presence of warm circumstellar material predominantly in the form of envelopes for Class I protostars and circumstellar disks for Class II stars. ii) Class III sources (mostly to be identified with WTTS) are distinctly different from lower classes by not revealing optically thick disks or signatures of accretion. iii) Star formation has been ongoing at a similar level during the past 1-2 Myr, with the Class-I protostars having ages of typically 0.1-0.2 Myr. iv) There is clear support for an evolutionary sequence Class I→II→III, although there is little luminosity evolution along with this sequence, indicating different evolutionary speeds for different objects. The infall time scale is a few times 10⁵ yrs, while the disk phase amounts to a few times 10⁶ yrs.

TMC has also been well-studied at millimeter wavelengths, having better high-resolution molecular line maps than any other star-forming region (*Onishi et al. 2002*). This region has been a major site for searches of complex molecules (*Kaifu et al., 2004*); many molecular transitions have been mapped across a large area, and the results will be interesting to compare with large-scale IR dust maps of the TMC (see Fig. 3 below).

In X-rays, TMC has again played a key role in our understanding of high-energy processes and circumstellar magnetic fields around pre-main sequence stars. Among the key surveys are those by *Feigelson et al. (1987), Walter et al. (1988), Bouvier (1990), Strom et al. (1990), Damiani et al. (1995)* and *Damiani and Micela (1995)* based on *Einstein Observatory* observations, and the work by *Strom and Strom (1994), Neuhäuser et al. (1995)* and *Stelzer and Neuhäuser (2001)* based on *ROSAT*. These surveys have characterized the overall luminosity behavior of TTS, indicated a dependence of X-ray activity on rotation, and partly suggested X-ray differences between CTTS and WTTS.

1.2 Is TMC Anomalous?

Although TMC has been regarded, together with the ρ Oph dark cloud, as the prototypical low-mass star-forming region, a few apparent peculiarities should be mentioned. TMC contains an anomalously large fraction of binaries (*Ghez et al., 1993*), compared with other SFRs (e.g., Orion) or with field stars. In TMC, about two thirds of all members are bound in multiple systems, with an average separation of about 0.3'' (e.g., *Leinert et al., 1993; Mathieu, 1994; Simon et al., 1995; Duchêne et al., 1999; White and Ghez, 2001; Hartigan and Kenyon, 2003*). Also, TMC cloud cores are comparatively small and low-mass when compared with cores in Orion or Perseus (*Kun 1998*).

TMC has also been found to be deficient of lowest-mass stars and BDs, with a mass distribution significantly enriched in 0.5–1 M_⊙ stars, compared to Orion samples (*Briceño et al., 2002*). The formation of BDs may simply be different in the low-density environment of TMC compared to the dense packing of stars in Orion.

Further, for reasons very poorly understood, TMC differs from other SFRs significantly with regard to X-ray properties. Whereas no X-ray activity-rotation correlation (analogous to that in main-sequence stars) is found for samples in the Orion star-forming regions, perhaps suggesting that all stars are in a saturated state (*Flaccomio et al., 2003a; Preibisch et al., 2005a*), the X-ray activity in TMC stars has been reported to decrease for increasing rotation period (e.g., *Neuhäuser et al., 1995; Damiani and Micela, 1995; Stelzer and Neuhäuser, 2001*). Also, claims have been made that the X-ray behavior of TMC CTTS and WTTS is significantly different, CTTS being less luminous than WTTS (*Strom and Strom, 1994; Damiani et al., 1995; Neuhäuser et al., 1995; Stelzer and Neuhäuser, 2001*). This contrasts with other star-forming regions (*Flaccomio et al., 2000; Preibisch and Zinnecker, 2001*), although recent reports re-

veal a similar segregation also for Orion and some other SFRs (Flaccomio *et al.*, 2003b; Preibisch *et al.*, 2005a). Some of these discrepancies may be due to selection and detection bias (e.g., WTTS are predominantly identified in X-ray studies, in contrast to CTTS).

2. NEW SURVEYS OF THE TAURUS CLOUDS

2.1 The Need for New Surveys

Some of the anomalies mentioned above may be strongly influenced by survey bias from the large size of TMC (25+ sq. degrees). For example, with the exception of IRAS and 2MASS, all the IR surveys of TMC focus on limited regions around dense molecular cloud cores of TMC (or of other star-forming regions) since these are easy to map using inefficient point-and-shoot strategies with small IR arrays. Systematic and deep investigations of more distributed low-mass star formation such as that in TMC are lacking. The exception in X-rays is the ROSAT All-Sky Survey obtained in the early nineties. However, this survey was of comparatively low sensitivity and recorded only rather soft X-ray photons, thus leaving all embedded sources and most of the lowest-mass stellar and BD population undetected. Angular resolution has also provided serious ambiguity.

A suite of new telescopes and satellite observatories now permits to reconsider the issues mentioned in Section 1. We have started a large multi-wavelength project to map significant portions of TMC in X-rays, the optical, near-infrared, and mid-infrared. The instruments used, *XMM-Newton* in X-rays, *Spitzer* in the near-/mid-infrared range, and the France-Canada-Hawaii Telescope (CFHT) in the optical range, provide an observational leap forward. Table 1 compares characteristic limitations of our surveys with limitations defined by previous instruments, represented here by the ROSAT Position-Sensitive Proportional Counter (PSPC All-Sky Survey for X-rays, *Neuhäuser et al.*, 1995; also some pointing observations, *Stelzer and Neuhäuser*, 2001), IRAS (25 μ m for mid-infrared data, *Kenyon and Hartmann*, 1995), and the KPNO 0.9 m telescope CCD surveys (for the optical, *Briceño et al.*, 1998, 2002; *Luhman* 2000; *Luhman et al.* 2003; *Luhman* 2004).

2.2 Scientific Goals of the New Surveys

2.2.1 The XMM-Newton X-Ray Survey. Our *XMM-Newton* X-ray survey maps approximately 5 sq. degrees (Fig. 1) of the denser molecular cloud areas with limiting sensitivities around $L_X \approx 10^{28}$ erg s $^{-1}$, sufficient, for the first time, to detect nearly every lightly absorbed, normal CTTS and WTTS and a significant fraction of BDs and protostars. The goals of this survey are:

1. To collect X-ray spectra and light curves from a statistically meaningful sample of TMC objects, and to characterize them in terms of X-ray emission measure distributions, temperatures, X-ray luminosities, and variability.
2. To interpret X-ray emission in the context of other stellar properties such as rotation, mass accretion and outflows.

Table 1: Characteristics of previous and new TMC surveys

Parameter	Previous surveys	New surveys
Luminosity detection limit:		
X-rays [erg s $^{-1}$]	$\approx 10^{29}$	$\approx 10^{28}$
mid-IR [L_\odot]	> 0.1	0.001
optical ^a [L_\odot]	$\approx 10^{-3}$	$\approx 10^{-4}$
Flux detection limit:		
X-rays [erg cm $^{-2}$ s $^{-1}$]	$\approx 4 \times 10^{-14}$	$\approx 4 \times 10^{-15}$
mid-IR [24 μ m, mJy]	500	1.2
optical [I, mag]	≈ 21	≈ 24
Mass detection limit:		
X-rays	$\approx 0.1 M_\odot$	$\approx 0.05 M_\odot$
mid-IR, 24 μ m	$\approx 0.5 M_\odot$	$\approx 1 M_{\text{Jup}}$
optical ^a	$\approx 15 - 20 M_{\text{Jup}}$	$\approx 10 M_{\text{Jup}}$
Accessible object types: ^b		
X-rays	II,III	I-III, BD, (HH)
mid-IR	0-III	0-III, BD, Ph, DD
optical	I-III, BD	I-III, BD
Angular resolution (FWHM, resp. pixel size):		
X-rays	$\approx 25''$	$\approx 4.5''$
mid-IR, 24 μ m	$1' \times 5'$	$\approx 6''$
optical	$\approx 0.67''/\text{pix}$	$\approx 0.2''/\text{pix}$
Energy or wavelength range:		
X-rays [keV]	0.1-2.4	0.2-15
mid-IR [μ m]	1.2-100	3.6-160
optical [nm]	800-1000	780-1170
Spectral resolution or filter width:		
X-rays [$E/\Delta E$]	≈ 1	$\approx 10-50^c$
mid-IR 24 μ m [$\Delta\lambda$]	5.8 μ m	4.7 μ m
Spatial extent:		
X-rays	all-sky	5 sq. deg
mid-IR	all-sky	30 sq. deg
optical	12.4 sq. deg	34 sq. deg

^a derived from the DUSTY models of *Chabrier et al.*

(2000) for $A_V < 5$ mag and age < 5 Myr

^b IR classes; HH = Herbig-Haro, DD = debris disks,

Ph = photospheres (Class III)

^c X-ray gratings: ≈ 300 (selected targets)

3. To investigate changes in the X-ray behavior as a young stellar object evolves.
4. To obtain a census of X-ray emitting objects at the stellar mass limit and in the substellar regime (BDs).
5. To study in what sense the stellar environment influences the X-ray production, and vice versa.
6. To search for new, hitherto unrecognized TMC members.

The outstanding characteristics of the survey are its sensitivity, its energy resolution, and its energy coverage. The TMC population is detected nearly completely in the surveyed fields, thus suppressing potential bias that previous surveys may have been subject to. In particular, a significant fraction of the TMC BDs can now be studied and their high-energy properties put into context with T Tauri stars. Moderate energy resolution permits a detailed description of the thermal plasma properties together with the measurement of the absorbing gas columns that are located predominantly in the Taurus clouds themselves, and even in the immediate circumstellar environment in the case of strongly absorbed objects. Photoelectric absorption acts more strongly

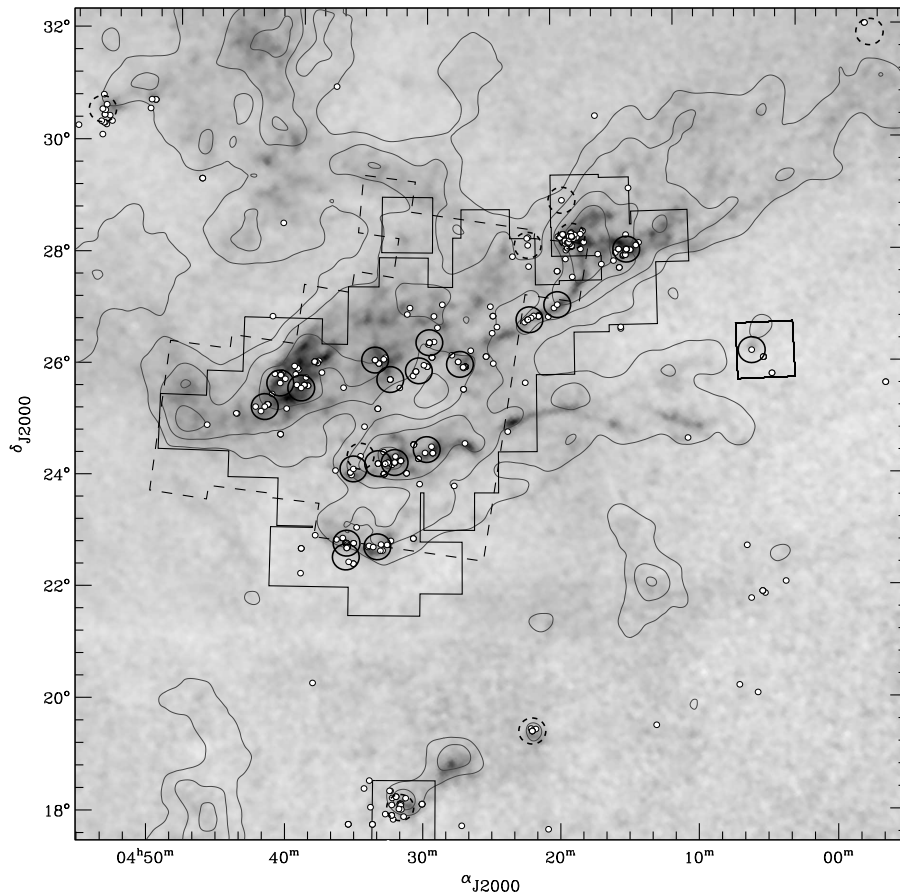


Fig. 1.— Map of the TMC region. The grayscale background map is an extinction (A_V) map from *Dobashi et al. (2005)*. The outlines of the CFHT and the *Spitzer* surveys are indicated by the solid and dashed polygons, respectively. The large (0.5 degrees diameter) circles show the fields of view of the *XMM-Newton* X-ray survey (the dashed circles marking fields from separate projects also used for the survey). Small white dots mark the positions of individual young stars. Note the outlying *XMM-Newton* fields around SU Aur (NE corner), ζ Per (NW corner), and L1551 and T Tau (south). (Figure courtesy of Nicolas Grosso.)

on the softer photons. ROSAT detected no TMC protostars because photons below 2 keV are almost completely absorbed. In contrast, harder photons to which *XMM-Newton* is sensitive penetrate large absorbing gas columns around protostars.

X-rays can be used to detect new candidate members of the TMC. We note in particular that WTTS are best identified through X-ray surveys (*Neuhäuser et al., 1995*). Placement on the HR diagram, X-ray spectral and temporal properties, and infrared photometry together can characterize new sources as being likely members of the association.

2.2.2 The *Spitzer* Infrared Survey. We have mapped the majority of the main TMC (≈ 30 sq. degrees, Fig. 1) using the *Spitzer* IRAC and MIPS instruments in order to take a deep census of young stars and disks to below the deuterium burning limit. These data play a crucial role in characterizing circumstellar material and BDs in our multiwavelength surveys of TMC. The goals are:

1. To survey the nearest example of a low-density star-forming region completely and objectively for stars and BDs.

2. To learn whether there is a “distributed” component of isolated star formation far removed from the multiple “centers” within the TMC complex.
3. To determine (via combination with ground-based data) what the distribution of stellar ages, masses and disk lifetimes are.
4. To carry out a definitive search for disks in transition between optically thick accretion disks and post-planet building disks and to use these data to constrain the timescales for planet building.
5. To discover which optical/2MASS/X-ray sources are the counterparts of known IRAS sources, as well as new *Spitzer* far-IR sources.

2.2.3 The CFHT Optical Survey. Our CFHT TMC survey was conducted as part of a larger-scale program targeted towards young galactic clusters (PI: J. Bouvier). It is a comprehensive, deep optical survey of the TMC down to 24 mag in I (23 in z) of 34 sq. degrees, covering most of the *XMM-Newton* and *Spitzer* fields (Fig. 1). The specific goals of the CFHT survey are:

1. To obtain a complete census of the low-mass star popu-

lation down to $I \simeq 22$, well into the substellar regime.

2. To obtain accurate optical I band photometry critical to derive fundamental parameters (reddening, luminosity estimates) for low-luminosity TMC members and investigate the occurrence of IR excesses.

3. To obtain deep images at sub-arcsecond resolution: 1) for a proper source identification, 2) to detect and map new large-scale HH flows and embedded envelopes.

These characteristics make the TMC CFHT survey the largest optical survey of the TMC sensitive well into the substellar regime. These data are critical for a proper identification of the sources and the determination of their fundamental parameters (effective temperature, reddening, luminosities). In particular, they play a central role in the detection and characterization of the TMC substellar population.

3. SURVEY STRATEGIES AND STATUS

3.1 The *XMM-Newton* Survey

Our *XMM-Newton* survey comprises 19 exposures obtained coherently as part of a large project (Güdel *et al.*, 2006a), complemented by an additional 9 exposures obtained in separate projects, bringing the total exposure time to 1.3 Ms. The former set of exposures used all three EPIC cameras in full-frame mode with the medium filter, collecting photons during approximately 30 ks each. Most of the additional fields obtained longer exposures (up to 120 ks) but the instrument set-up was otherwise similar. The spatial coverage of our survey is illustrated in Fig. 1. The survey includes approximately 5 sq. degrees in total, covering a useful energy range of $\approx 0.3 - 10$ keV with a time resolution down to a few seconds. The circular fields of view with a diameter of 0.5 degrees each were selected such that they cover the densest concentrations of CO gas, which also show the strongest accumulations of TMC stellar and substellar members. We also obtained near-ultraviolet observations with the Optical Monitor (OM), usually through the U band filter, and in exceptional cases through filters at somewhat shorter wavelengths. The OM field of view is rectangular, with a side length of $17'$. An on-axis object could be observed at high time resolution (0.5 seconds).

Data were processed using standard software and analysis tools. Source identification was based on procedures involving maximum-likelihood and wavelet algorithms. In order to optimize detection of faint sources, periods of high background local particle radiation levels were cut out.

A typical exposure with an average background contamination level reached a detection threshold of $\approx 9 \times 10^{27}$ erg s $^{-1}$ on-axis and $\approx 1.3 \times 10^{28}$ erg s $^{-1}$ at $10'$ off-axis for a lightly absorbed X-ray source with a thermal spectrum characteristic of T Tau stars (see below) subject to a hydrogen absorption column density of $N_H = 3 \times 10^{21}$ cm $^{-2}$. This threshold turns out to be appropriate to detect nearly every T Tau star in the surveyed fields.

We interpreted all spectra based on thermal components combined in such a way that they describe emission

measure distributions similar to those previously found for nearby pre-main sequence stars or active zero-age main sequence stars (Telleschi *et al.*, 2005; Argiroffi *et al.*, 2004; Garcia *et al.*, 2005; Scelsi *et al.*, 2005). An absorbing hydrogen column density was also fitted to the spectrum.

3.2 The *Spitzer* Survey

In order to study material around very low-mass young stars and BDs, we require the use of both the *Spitzer* imaging instruments (IRAC and MIPS). The short IRAC bands detect the photospheres of BDs and low mass stars. Using the models of Burrows *et al.* (2003), we find that 2–12 s exposures are required to detect BDs down to $1 M_{\text{Jup}}$ in the $4.5 \mu\text{m}$ IRAC band (see Table 2). Young BDs without disks will require spectroscopic confirmation since they will resemble M stars. The exquisite sensitivity of IRAC also makes it susceptible to saturation issues for the solar-type population of the Taurus clouds. In order to mitigate these effects, we have observed with the “high dynamic range” mode which obtains a short (0.4 s) frame together with a 10.4 s one. Total IRAC and MIPS sensitivities for our maps are listed in Table 2, together with the number of independent exposures performed per point in the map (data redundancy). Disks are indicated by measured flux densities well above photospheric levels and/or stellar colors inconsistent with a Rayleigh-Jeans spectrum between any pair of bands. The presence of disks is revealed by comparison of the 8 and $24 \mu\text{m}$ bands to each other and the shorter IRAC bands. For MIPS, we chose fast scan for efficient mapping at $24 \mu\text{m}$. The resulting 1.2 mJy 5σ sensitivity for MIPS $24 \mu\text{m}$ enables detection of disks $20\times$ fainter than the low-luminosity edge-on disk HH 30 IRS (Stapelfeldt *et al.*, 1999). This is sufficient to detect \geq few M_{Jup} disks around $\geq 0.007 M_{\odot}$ 3 Myr old BDs (Evans *et al.*, 2003).

Due to the proximity of TMC, it subtends an area of more than 25 sq. deg on the sky. *Spitzer* is the first space observatory with modern sensitivity which possesses the observing efficiency to map the region as a single unit within a feasible observing time. Our observing program attempted to survey the TMC nearly completely and objectively within a limited time (134 hours). In particular, we chose our coverage of TMC (illustrated in Fig. 1) to overlap as many CFHT and *XMM-Newton* pointings as possible while mapping all the known contiguous ^{13}CO cloud. In addition, in order to obtain imaging of the Heiles 2 and Lynds 1536 clouds most efficiently by mapping in long strips, we obtained a considerable portion of adjacent off-cloud area south of the TMC. This region is invaluable for assessing the distribution of sources with excess off the cloud, as well as galactic and extragalactic contamination. The MIPS data were obtained using the scan mapping mode (Rieke *et al.*, 2004) which uses a cryogenic mirror to perform image motion compensation for short exposures while the telescope is slewing. The “fast scan” mode is by far the most efficient way for *Spitzer* to map large areas quickly, covering more than 1 sq. degree per hour. Due to the lack of an internal

scan mirror, IRAC maps at the slow speed of 0.33 sq. degrees per hour at the minimal depth of our survey. Because each point in the IRAC map has a total redundancy of only two exposures, cosmic ray removal is difficult.

Since TMC is located virtually on the ecliptic plane, we mapped twice at 8 and 24 μm to identify asteroids. A waiting period of 3–6 hr between mapping epochs allowed asteroids with a minimum motion of 3.5''/hour to move enough so that they can be identified by comparing images from the two epochs. Initial results suggest there are several thousand asteroids detected in our maps. These will be eliminated from the catalog of young stellar objects. However, our strategy enables a statistical asteroid study with the largest low ecliptic latitude survey yet envisioned for *Spitzer*.

Table 2: *Spitzer* TMC survey estimated sensitivity

Instrument	Band (μm)	5σ Point Source Sensitivity (mJy)	Redundancy
MIPS	24	1.2	10
MIPS	70	~ 44	5
MIPS	160	~ 500 ; 2.64 MJy/sr	~ 1
...	...	(extended source)	(bonus band)
IRAC	3.6	0.017	2
IRAC	4.5	0.025	2
IRAC	5.8	0.155	2
IRAC	8.0	0.184	2

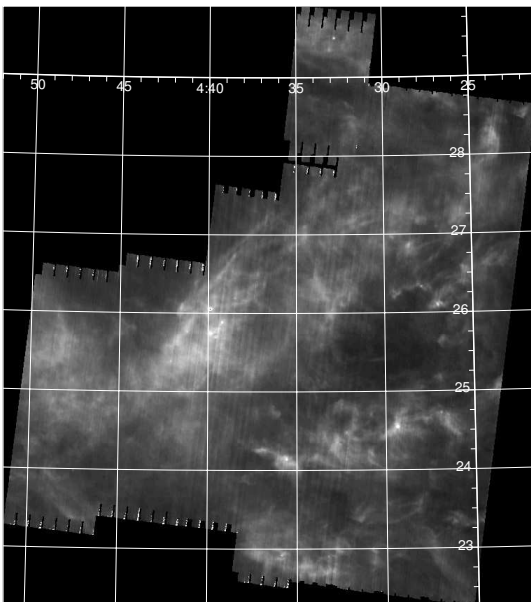


Fig. 2.— 29 square degree MIPS 160 μm map of nearly the entire TMC region observed in the *Spitzer* TMC survey. The brightest regions reach an intensity of over 200 MJy/sr. The image has been slightly smoothed to fill in some narrow gaps in coverage. Effective exposure time is about 3 seconds.

Spitzer observations of TMC were performed in February and March of 2005. Although the bulk of the data were released to the team in May, the field which includes Lynds

1495 remains embargoed until March 2006. The team has spent several months in 2005 developing algorithms to mitigate remaining instrumental signatures in the data, many of which are aggravated by the presence of bright point sources and extended nebosity. Removal of radiation artifacts from the IRAC data has been a considerable challenge due to the minimal repeat coverage of our mapping strategy. However, as of PPV, a prototype reprocessing code has been implemented for IRAC. Using this software and a robust mosaicing algorithm which uses the short HDR frame to eliminate the brightest cosmic rays, a 1.5 square degree region centered around 04^h 26^m 10.9^s +27° 18' 10'' (J2000) has been fully reprocessed in the IRAC and MIPS bands, source extracted, and bandmerged. The MIPS 24 μm data are most affected by the presence of thousands of asteroids, which outnumber the stars at this wavelength. It is therefore necessary to separately extract sources from each of the MIPS 24 μm observing epochs, then bandmerge these lists to achieve a reliable source list minus asteroids. One of the most interesting preliminary data products is a complete 160 μm map of the entire available TMC region (29 square degrees). This map is presented in Fig. 2. The areas of brightest 160 μm emission correspond well to the ¹³CO clouds.

3.3 The CFHT Survey

The CFHT TMC survey has been performed in 4 successive periods on the Canada-France-Hawaii Telescope with the CFH12k and MEGACAM large-scale optical cameras (see Table 3 for a detailed journal). Taking into account overlapping fields, a total effective surface of 34 sq. degrees has been surveyed down to an I band sensitivity limit of $I_C = 24$, i.e., well into the substellar regime (see below). It encompasses more than 80% of the known *stellar* population. This is to date the largest optical survey of the TMC sensitive well into the substellar regime. The outline of the survey, overlaid on the CO gas density map, is presented in Fig. 1 together with the known TMC population.

The technical characteristics of the CFH12k and MEGACAM cameras are presented in *Cuillandre et al.* (2000) and *Boulade et al.* (2003), respectively. The first half of the CFH12k survey (centered on the densest part of TMC, from 1999 to 2001), has been obtained as part of CFHT director's discretionary time, while the remaining larger set of data has been obtained, in service mode, as part of a larger key program devoted to the study of young clusters. Currently, 28 of the total 34 sq. deg have been reduced and analyzed. We refer below to this as the primary CFHT survey. Data reduction, performed at CFHT using elements of the Elixir system (*Magnier and Cuillandre, 2004*), included bias and dark subtraction, flat-fielding, fringing correction, bad pixel removal and individual frame combination. Point source detection was performed on the combined $I + z'$ images. For the CFH12k data, PSF fitting photometry was extracted with the PSFex routine from the SExtractor program (*Bertin and Arnouts, 1996*), while aperture photometry was

Table 3: Overview of the CFHT optical survey of the Taurus cloud

Instrument	FOV (deg ²)	Pixel ("'/pixel)	Date	Area (deg ²)	Band	Completeness limit	Mass limit ($A_V=5$, 5Myr)
CFHT12k	0.33	0.21	1999-2001	3.6	R, I, z'	23, 22, 21	15 M_J
CFHT12k	0.33	0.21	2002	8.8	I, z'	22, 21	15 M_J
Megacam	1	0.19	2003-2004	34	i', z'	24, 23	10 M_J

obtained for the MEGACAM data with the same program. Photometric catalogs were combined, using the transformation between CFHT12k (I, Z') and MEGACAM (i', z') photometric systems, computed with overlapping fields. The survey yielded more than 10^6 sources detected down to $I = 24$ and $z' = 23$. From the turn-over at the faint end of the magnitude distribution, we estimate the completeness limits of our optical photometric survey to be $I = 21.8$ and $z' = 20.9$, which corresponds to a mass completeness limit of $15 M_{Jup}$ for $A_V < 5$ and age < 5 Myr, according to the pre-main sequence DUSTY models of *Chabrier et al.* (2000). On the bright side, the saturation limits are $i' = 12.5$ and $z' = 12$. Follow-up studies at NIR wavelengths (1–2 μm) are planned. As part of the UKIRT Infrared Deep Sky Survey most of the MEGACAM fields will be observed down to $K = 18$.

4. OVERVIEW OF THE POPULATION

4.1 Fundamental Parameters

We have compiled a comprehensive catalog of all sources thought to be members of the TMC, collecting photometry, effective surface temperature, bolometric luminosities of the stars, L_* , derived mostly from near-IR photometry (see, e.g., *Briceño et al.*, 2002), extinctions A_V and A_J , masses, radii, $H\alpha$ equivalent widths, rotation periods and $v \sin i$ values, mass accretion and outflow rates, and some further parameters from the published literature.

There is considerable spread in some of the photometry and A_V (or A_J) estimates for a subsample of stars, resulting in notable differences in derived L_* and masses. We have coherently re-derived ages and masses from the original L_* and T_{eff} using *Siess et al.* (2000) evolutionary tracks. For the final list of parameters, we have typically adopted the values in the recent compilation by *Briceño et al.* (2002) or, if not available, the catalogs of *Kenyon and Hartmann* (1995) and *Briceño et al.* (1998). Binary component information is mostly from *White and Ghez* (2001) and *Hartigan and Kenyon* (2003). Further parameters were complemented from the studies by *Luhman et al.* (2003), *Luhman* (2004), *White and Hillenbrand* (2004), and *Andrews and Williams* (2005).

4.2 Known Protostellar and Stellar Population

The bright protostellar and stellar population of TMC has long been studied in the infrared. *Strom et al.* (1989) concluded that about half of the young stellar population of

TMC above $1 L_\odot$ were surrounded by optically thick disks as demonstrated by their IRAS detections. This work was extended and complemented by the work of *Kenyon and Hartmann* (1995) who added fainter association members and ground-based photometry out to 5 μm to the SEDs. ISOCAM observed the L1551 field in the southern TMC, detecting an additional 15 YSO candidates (*Galfalk et al.*, 2004). *Spitzer* IRAC photometry of 82 known Taurus association members is reported in *Hartmann et al.* (2005). This study finds that the CTTS are cleanly separated from the WTTS in the [3.6]-[4.5] vs. [5.8]-[8.0] color-color diagram. The WTTS are tightly clustered around 0 in both colors, and the CTTS form a locus around [3.6]-[4.5] ≈ 0.5 and [5.8]-[8.0] ≈ 0.8 . A similar conclusion is reached by *Padgett et al.* (2006, submitted) who obtained pointed photometry of 83 WTTS and 7 CTTS in Taurus, Lupus, Chamaeleon, and Ophiuchus at distances of about 140 - 180 pc, with ages most likely around 0.5–3 Myr. They find that only 6% of WTTS show excess at 24 μm , with a smaller percentage showing IRAC excesses. Unfortunately, it is currently not possible in every case to distinguish a true WTTS (pre-main sequence star without strong $H\alpha$ emission) from X-ray bright zero-age main-sequence stars projected onto the cloud. Thus, current samples of WTTS and possibly “weak” BDs may be contaminated with older objects, skewing the disk frequency for these sources.

Class I “protostars” are perhaps more easily studied in TMC than elsewhere due to the lack of confusion in the large long wavelength IRAS beams. One troubling aspect of the placement of Class Is in the standard picture of star formation (*Adams et al.* 1987) is that the TMC Class Is typically show luminosities no higher than, and in many cases lower than, the Class II T Tauri stars (*Kenyon and Hartmann*, 1995). This issue has led to controversy regarding whether Class I sources are at an earlier evolutionary state than Class II T Tauri stars (*Eisner et al.*, 2005; *White and Hillenbrand*, 2004). It is hoped that *Spitzer* can boost the number of known Class I sources and elucidate their spectral properties, helping to determine the true nature of these objects.

4.3 X-Ray Sources

The detection statistics of our X-ray survey is summarized in Table 4 (we have added one brown-dwarf detection from a complementary *Chandra* field). An important point for further statistical studies is that the X-ray sample of detected CTTS and WTTS is nearly complete for the

surveyed fields (as far as the population is known). The few remaining, undetected objects are either heavily absorbed, have unclear YSO classification, are objects that have been very poorly studied before, or are very-low mass objects. Some may not be genuine TMC members. In contrast, previous X-ray surveys did not detect the intrinsically fainter TTS population, potentially introducing bias into statistical correlations and population studies. It is little surprising that some of the protostars remained undetected given their strong photoelectric absorption. The detection rate of BDs (53%) is also very favorable; the remaining objects of this class are likely to be intrinsically fainter than our detection limit rather than being excessively absorbed by gas (A_V of those objects typically being no more than few magnitudes).

Table 4: X-ray detection statistics

Object type	Members surveyed	Detections	Detection fraction
Protostars	20	9	45%
CTTS	62	54	87%
WTTS	49	48	98%
BDs	19	10	53%

X-rays can efficiently be used to find new candidate TMC association members if X-ray information (luminosity, temporal and spectral characteristics) is combined with information from the optical/near infrared (placement on the HR diagram, L_* , age) and from the mid-infrared (presence of disks or envelopes). *Scelsi et al.* (2006, in preparation) have thus identified several dozens of potential candidates of the TMC population. Follow-up studies will be needed to confirm these candidates.

4.4 Bright $24 \mu\text{m}$ Sources

The scientific goal of the TMC *Spitzer* survey is to obtain a complete census of the stellar content of these clouds down to the hydrogen burning limit. Our *Spitzer* maps have sufficient sensitivity to detect $1 M_{\text{Jup}}$ young BDs and optically thin disks around solar-type stars at the distance of TMC. However, a complication of our survey is that the small size of *Spitzer* limits its spatial resolution, making the task of distinguishing faint stars from galaxies difficult, especially in the presence of optical extinction. Unfortunately, the IR spectral energy distributions of extincted stars with infrared excesses strongly resemble the SEDs of IR-bright galaxies (*Evans et al.*, 2003). Experience with the galactic First Look Survey (*Padgett et al.*, 2004) and the c2d Legacy program (cf. *Young et al.*, 2005) have shown that strong $24 \mu\text{m}$ emission is an excellent signpost of young stellar objects. The extragalactic *Spitzer* surveys performed by the GTOs and the Extragalactic First Look Survey have established that extragalactic sources dominate the sky at a flux level of 1 mJy at $24 \mu\text{m}$, but are fewer than 1 per square degree at 10 mJy (*Papovich et al.*, 2004). Thus, in a region of known star formation, strong $24 \mu\text{m}$ sources

are more likely to be galactic than extragalactic sources. Although our analysis of the TMC *Spitzer* maps is incomplete, we have assembled SEDs for the bright (≥ 10 mJy) $24 \mu\text{m}$ sources over more than 15 square degrees. About 100 sources were found in this preliminary list, of which 56 have no SIMBAD identifier. By analogy with SEDs of the known young stellar objects of the cloud which were also recovered by this technique, we believe that some of the previously unknown $24 \mu\text{m}$ sources may represent the brightest stars with disks among the YSOs which were too faint for IRAS to detect. SEDs for four of the new bright $24 \mu\text{m}$ sources are presented in Fig. 3.

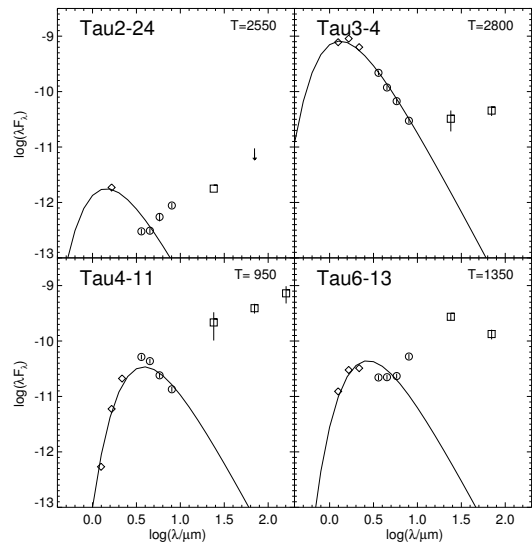


Fig. 3.— 2MASS NIR + *Spitzer* IRAC and MIPS spectral energy distributions of four bright $24 \mu\text{m}$ sources discovered in the course of the survey. Temperatures indicated in the plots are effective temperatures of the plotted photosphere.

5. THE SUBSTELLAR SAMPLE

The TMC is a particularly interesting target for searches of young substellar objects. It has a large extension, so it can be studied for ejection effects; there are no bright stars there to irradiate and disturb the stellar surroundings; the census of stellar members is relatively complete down to M2V spectral types (*Kenyon & Hartmann*, 1995), and its spatial distribution is known (*Gómez et al.*, 1993). The average low extinction ($A_V = 1$) associated with this cloud as well as its young age combine to provide a high sensitivity to very low-mass objects in the optical domain. However, its large spatial extent ($\simeq 100$ square degrees) requires mapping an extensive area. Significant breakthrough in this domain has been made possible with the recent availability of large scale optical cameras.

Searches for substellar objects, by *Briceño et al.* (1998) *Luhman* (2000), *Briceño et al.* (2002), *Luhman et al.* (2003), *Luhman* (2004) and references therein, have revealed a factor of 1.4 to 1.8 deficit of BDs with respect

to stars in TMC compared to the Trapezium cluster. This result has been interpreted as an indication that sub-stellar object formation depends on the environment. However, all these previous studies were concentrated on the immediate vicinity of the high stellar density regions. If BDs are stellar embryos ejected from their birth sites early in their evolution as proposed by *Reipurth and Clarke (2001)*, a significant fraction of the substellar content of the central parts of the cloud could have scattered away and may have been missed. This being the main scientific driver of the CFHT survey, we describe recent CFHT results from the search for substellar objects in TMC based on *Martín et al. (2001)* and *Guieu et al. (2006)* below, together with aspects from *Spitzer* and *XMM-Newton*.

5.1 New TMC Very Low-Mass Members

Substellar photometric candidates are identified from their location in combined optical/NIR color-magnitude and color-color diagrams (see Fig. 4). The full details of the selection process are given in *Guieu et al. (2006)*. Complementary near-infrared photometry, taken from the 2MASS catalog, is critical to reduce the strong expected galactic contamination, primarily from background giants. Residual contamination is still expected to be at the 50 % level. In order to properly assess TMC membership, spectroscopic follow-up of the photometrically selected candidates is therefore mandatory. The criteria used to assess TMC membership are detailed in *Guieu et al. (2006)*. They rely on estimates of the surface gravity, obtained both from spectral fitting and measurements of the Na I equivalent widths. The level of H α emission is used as an additional indicator of youth. At the median age of the TMC population of 3 Myr, the pre-main sequence models of *Chabrier et al. (2000)* predict the stellar/substellar boundary to lie at a spectral type between M6 and M6.5V.

The photometric selection procedure yielded, over the primary 28 sq. degrees CFHT survey, 37 TMC mid- to late-M spectral type new candidate members with $i' < 20$ (magnitude limit set to allow a proper spectral type determination). TMC membership has been confirmed spectroscopically for 21 of these sources (*Martín et al. 2001*, *Guieu et al. 2006*), 16 of which have spectral types later than M6.5V, i.e. are likely substellar. These new findings bring to 33 the current published census of TMC BDs, thus allowing for a preliminary statistical study of their properties.

5.2 A Peculiar Substellar IMF in TMC?

When all published optical surveys are combined, the census for very low-mass TMC objects is now complete down to $30 M_{\text{Jup}}$ and $A_V \leq 4$ over an effective surface area of 35 sq. deg ($\approx 30\%$ of the total cloud surface). This mass completeness, derived from the DUSTY model of *Chabrier et al. (2000)*, is set both by the 2MASS completeness limits (J=15.25, H=14.4, K=13.75) and the typical sensitivity limit of optical spectroscopic observations ($i' \leq 20$).

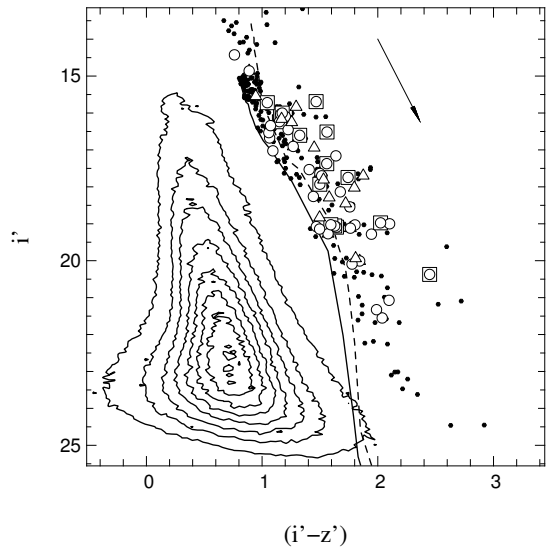


Fig. 4.— Observed $i'/(i' - z')$ color-magnitude diagram used to select low-mass TMC candidates. Small black dots are candidate TMC members. The photometric mid to late-M candidates observed spectroscopically by *Guieu et al. (2006)* are displayed by black open circles. Triangles are previously known TMC members. Squares identify the spectroscopically confirmed 21 new TMC members from *Guieu et al. (2006)* and *Martín et al. (2001)*. The two steep solid curves show the locations of the 1 Myr and 10 Myr isochrones from the DUSTY model of *Chabrier et al. (2000)* at the TMC distance. The arrow indicates a reddening vector of $A_V = 4$ magnitudes. Figure adapted from *Guieu et al. (2006)*.

Briceño et al. (2002) have introduced the substellar-to-stellar ratio

$$R_{ss} = \frac{N(0.03 < M/M_{\odot} < 0.08)}{N(0.08 < M/M_{\odot} < 10)}$$

as a measure of the relative abundance of BDs. In their pioneering study, targeted towards the high-density aggregates, *Briceño et al. (2002)* determined a value of R_{ss} (0.13 ± 0.05) lower by a factor 2 than the one found in the Trapezium cluster. This study thus suggested that the relative abundance of BDs in star-forming regions may depend on initial conditions, such as the stellar density. However, in a recent, more extensive study covering 12 square degrees, *Luhman (2004)* found that the BD deficit in TMC (with respect to Orion) could be less pronounced than previously thought. Combining the recent new members from the CFHT survey with previously published results, *Guieu et al. (2006)* derive an updated substellar-to-stellar ratio in TMC of $R_{ss} = 0.23 \pm 0.05$. This value is now in close agreement with the Trapezium value of $R_{ss}(\text{Trapezium}) = 0.26 \pm 0.04$ estimated by *Briceño et al. (2002)*, using the same evolutionary models and treating binary systems in the same manner. It also appears consistent with the more recent values derived for IC 348 by *Slesnick et al. (2004)*, the Pleiades

by *Moraux et al.* (2003) and computed from the galactic disk system IMF of *Chabrier* (2003) (see *Monin et al.*, 2005, for a compilation of these values). These new findings seem to suggest a universal 20–25% value for the relative abundance of BDs in young clusters. The fact that the estimate of the substellar-to-stellar ratio in TMC has kept increasing as larger areas were surveyed suggests that this ratio may depend on the local stellar density. Indeed, *Guieu et al.* (2006) find evidence for a deficit of the abundance of BDs of a factor $\simeq 2$ in the central regions of the TMC aggregates (on scales of $\simeq 0.5$ pc) with respect to the more distributed population. As discussed in *Guieu et al.* (2006), this result may be an indication for spatial segregation resulting from ejection of the lowest-mass members and seem to favor dynamical evolution of small N body systems as the formation process of substellar objects (see *Guieu et al.* 2006 for a full discussion).

5.3 X-Ray Properties of TMC BDs

The area surveyed by the 28 pointings of *XMM-Newton*, combined with one *Chandra* archival observation, allow us to study the X ray emission of 19/33 TMC BDs (*Grosso et al.*, 2006a). Among these, ten BDs are detected, yielding a detection rate of $\approx 53\%$. One BD displayed an impulsive flare, demonstrating variability in X-rays over periods of a few hours. The detection rate of TMC BDs thus appears similar to the one in Orion where it reaches $\approx 50\%$ for $A_V < 5$ (*Preibisch et al.*, 2005b). As in Orion, there is a tendency to detect earlier (hotter) BD, with spectral types earlier than M7–M8.

There is appreciable scatter in the X-ray luminosities. The most luminous examples show L_X of order $\approx 10^{29}$ erg s $^{-1}$. No trend is seen for L_X/L_* with spectral type, i.e., the efficiency of magnetic field production and coronal heating appears to be constant in low-mass stellar and substellar objects (Fig. 5).

5.4 Disk and Accretion Properties of TMC BDs

There is now ample evidence that TMC BDs experience accretion processes similar to the more massive TTS. Near-infrared L band excesses have been detected in TMC substellar sources, indicating a disk frequency of $\approx 50\%$ (*Liu et al.*, 2003; *Jayawardhana et al.*, 2003). Broad asymmetric $H\alpha$ emission profiles characteristic of accretion are reported in a few TMC BDs (*Jayawardhana et al.*, 2002, 2003; *White and Basri*, 2003; *Muzerolle et al.*, 2005, and references therein; *Mohanty et al.*, 2005). Extending the study of *Barrado y Navascues and Martín* (2003), *Guieu et al.* (2006) find that the fraction of BDs in TMC with levels of $H\alpha$ emission in excess of chromospheric activity to be 42%, similar to the low-mass TTS.

Of the twelve BD candidates optically selected from the CFHT survey, half have strong excesses in the infrared as measured from *Spitzer* data (*Guieu et al.* 2005). Most of these diverge from the predicted photospheric fluxes at

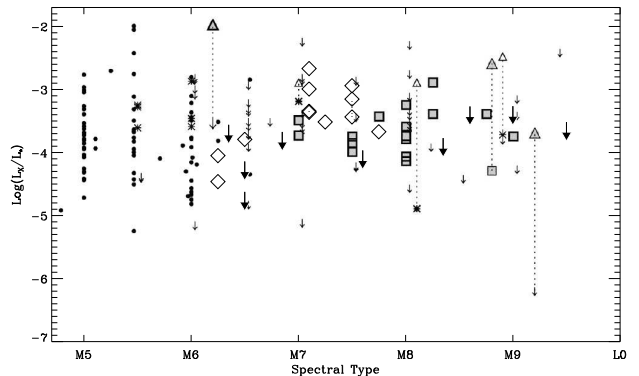


Fig. 5.— L_X/L_* of low-mass stars and BDs as a function of spectral class, including samples of late-type main-sequence field stars (asterisks, *Fleming et al.*, 1993), the Orion Nebula Cluster BD sample (filled squares, triangles, and small arrows) and T Tauri stars later than M5 (filled dots) from *Preibisch et al.* (2005b), and our sample of TMC detections (diamonds) and upper limits (arrows). (Figure courtesy of Nicolas Grosso.)

$5.8 \mu\text{m}$, and all six are strongly detected at $24 \mu\text{m}$. The other substellar candidates have IRAC fluxes indistinguishable from a late-M photosphere, and only one is detected at $24 \mu\text{m}$. These results are similar to those found for TMC BD in the literature by *Hartmann et al.* (2005). Both studies find that the BD with excess (“Classical” BD or CBD) have disk properties indistinguishable from classical T Tauri stars. Similarly, the “weak” BDs have purely photospheric colors similar to the WTTS. Further analysis and modeling is required to determine whether the “classical” BDs have unusually flat disks as suggested by *Apai et al.* (2002).

There is support for BD variability in the U-band observations obtained simultaneously by the Optical Monitor (OM) onboard *XMM-Newton*. The OM observed 13 of the 19 X-ray surveyed BDs in the U-band. Only one BD was detected, 2MASS J04552333+3027366, for which the U band flux increased by a factor of about 2–3 in ≈ 6 hours (Fig. 6; *Grosso et al.*, 2006b). The origin of this behavior can be explained by several different mechanisms: either rotational modulation of a hot or dark spot, or a coronal magnetic flare, or variable accretion. This BD was not detected in X-rays at any time. It is known to accrete at a rate of $10^{-10} M_\odot \text{ yr}^{-1}$ (*Muzerolle et al.*, 2005). Assuming that the relation $\log L_{\text{acc}} \propto \log L_U$ that applies to TTS (*Gullbring et al.*, 1998) is also valid for BDs, the accretion rate must have increased by a factor of about 2–3 during the observing time to explain the increase observed in the U-band.

All these results argue for a continuous M/\dot{M} relation through the stellar/substellar boundary, as illustrated e.g. in Fig. 5 of *Muzerolle et al.* (2005).

5.5 Implication for Substellar Formation Model

The fact that the abundance of BDs (down to $30 M_{\text{Jup}}$)

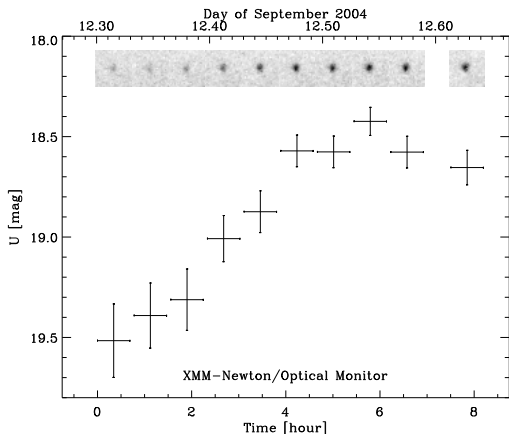


Fig. 6.— U-band light curve of 2MASS J04552333+3027366 during an *XMM-Newton* observation. The slow increase may be ascribed to an accretion event. The insets show U-band images from which the fluxes have been extracted. Background limiting magnitudes are indicated by thick horizontal lines (*Grosso et al.*, 2006b).

relative to stars is found to be the same ($\approx 25\%$) in the diffuse TMC and in the high-density Orion Nebula Cluster seems to suggest that there is no strong dependency of the substellar IMF on initial molecular cloud conditions, in particular gas density and level of turbulence. This fact and the increase of the BD abundance with decreasing stellar density found by *Guieu et al.* (2006) could be best explained if a fraction of the distributed population in TMC is formed of low-mass stars and substellar objects ejected from the aggregates through rapid dynamical decay in unstable small N-body systems (*the ejected-embryo model*). Indeed, such a result is predicted by the dynamical evolution studies of *Kroupa and Bouvier* (2003) and the recent sub-sonic turbulent fragmentation simulations of *Goodwin et al.* (2004). For a detailed discussion, see *Guieu et al.* (2006) and *Monin et al.* (2006).

It has often been argued that the presence of accretion / outflow activity in BDs would be incompatible with an ejection formation scenario. However, even truncated disks in ejected objects can survive for a few Myr, a period consistent with the TMC age. The viscous timescale of a disk around a central mass M varies as $M^{-1/2}$, so for a disk truncated at $R_{\text{out}} = 10$ AU, $\tau_{\text{visc}} \approx 2$ Myr around a $50 M_{\text{Jup}}$ BD (for $\alpha \approx 10^{-3}$ at 10 AU). Furthermore, an accretion rate of $\dot{M} = 10^{-11} M_{\odot} \text{yr}^{-1}$ and a disk mass of $10^{-4} M_{\odot}$ results in a similar lifetime of a few Myr. So, there is no contradiction between BD ejection and the presence of (possibly small) accretion disks at a few Myr age.

6. X-RAYS AND MAGNETIC ACTIVITY

6.1 X-Ray Luminosity

Fig. 7 shows the distribution of the ratio between X-ray luminosity L_X and (stellar, photospheric) bolometric luminosity L_* as a function of L_* (the latter derived from

optical or near-IR data, see Section 4.1 for references) for all spectrally modeled TTS and protostars, and also including the *detected* BDs (we exclude the peculiar sources discussed in Section 6 below; some objects were observed twice with different L_X - we use the logarithmic averages of L_X in these cases). We do not give errors for L_X because most objects are variable on short and long time scales (hours to days), typically within a factor of two outside obvious, outstanding flares. Most stars cluster between $L_X/L_* = 10^{-4} - 10^{-3}$ as is often found in star-forming regions (*Güdel* 2004 and references therein). The value $L_X/L_* = 10^{-3}$ corresponds to the saturation value for rapidly rotating main-sequence stars (see below). We note a trend for somewhat lower levels of L_X/L_* for higher L_* (typically, more massive stars). What controls the X-ray luminosity level? Given the trend toward saturation in Fig. 7, one key parameter is obviously L_* . Although for pre-main sequence stars there is no strict correlation between L_* and stellar mass, it is interesting that we find a rather well-developed correlation between L_X and mass M (Fig. 8, masses derived from T_{eff} and L_* based on *Siess et al.* 2000 isochrones) that has been similarly noted in Orion (*Preibisch et al.*, 2005a). Part of this correlation might be explained by higher-mass stars being larger, i.e., providing more surface area for coronal active regions. The correlation between surface area and L_X is, however, considerably weaker than the trend shown in Fig. 8.

We plot in Fig. 9 the L_X/L_* distribution separately for CTTS and WTTS (*Telleschi et al.*, 2006, in preparation; the average L_X is used for objects observed twice). Because our samples are nearly complete, there is little bias by detection limits. The distributions are close to log-normal, and corresponding Gaussian fits reveal that WTTS are on average more X-ray luminous (mean of distribu-

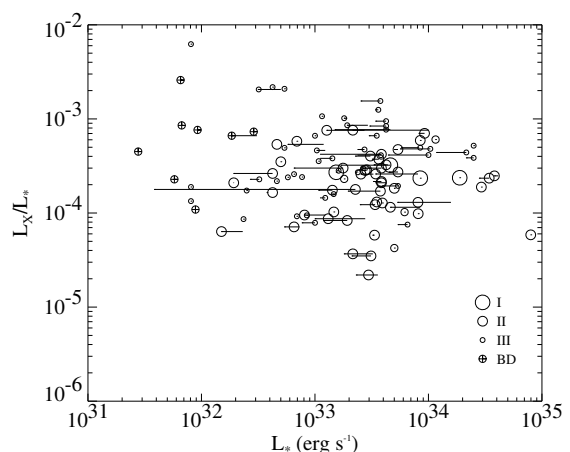


Fig. 7.— Plot of L_X/L_* as a function of L_* for all X-ray detected (and spectrally modeled) stars and BDs (but excluding Herbig stars). Symbol size, from largest to smallest: protostars (IR Class I) - CTTS (or IR Class II) - WTTS (or IR Class III). Circles with crosses: BDs. The error bars indicate ranges of L_* given in the literature.

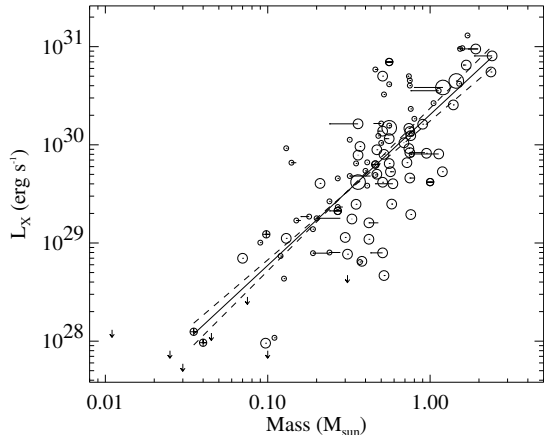


Fig. 8.— X-ray luminosity L_X versus stellar mass (excluding Herbig stars). A clear correlation is visible. Key to the symbols is as in Fig. 7 (after Telleschi *et al.*, 2006, in preparation).

tion: $\log L_X/L_* = -3.39 \pm 0.06$) than CTTS (mean: $\log L_X/L_* = -3.73 \pm 0.05$), although the widths of the distributions are similar. This finding parallels earlier reports on less complete samples (Stelzer and Neuhäuser, 2001), ruling out detection bias as a cause for this difference. A similar segregation into two X-ray populations has not been identified in most other SFRs (e.g., Preibisch and Zinnecker, 2001 - but see recent results on the Orion Nebula Cluster in Preibisch *et al.*, 2005a). The cause of the difference seen in TMC may be evolutionary (stellar size, convection zone depth), or related to the presence of accretion disks or the accretion process itself. We will return to this point in Section 6.3 below.

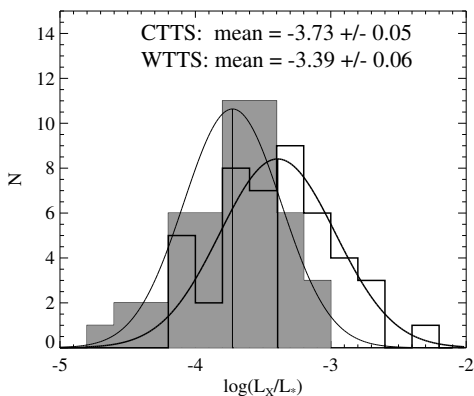


Fig. 9.— Comparison of the L_X/L_* distributions for CTTS (shaded histogram) and WTTS (solid), together with log-normal fits. The CTTS sample is on average less luminous (normalized to L_*) than the WTTS sample. The errors in the plot indicate the error of the means of the distributions (Telleschi *et al.*, 2006, in preparation).

6.2 Rotation and Activity

Rotation plays a pivotal role for the production of mag-

netic fields in main-sequence stars, and thus for the production of ionizing (ultraviolet and X-ray) radiation. The rotation period P is controlled by the angular momentum of the young star inherited from the contracting molecular cloud, by the further contraction of the star, but possibly also by magnetic fields that connect the star to the inner border of the circumstellar disk and thus apply torques to the star. Strictly speaking, in the standard (solar) $\alpha - \omega$ dynamo theory, it is *differential* rotation that, together with convection, produces magnetic flux near the boundary between the convection zone and the radiative core. Because the younger T Tau stars are fully convective, a dynamo of this kind is not expected, but alternative dynamo theories based entirely on convective motion have been proposed (e.g., Durney *et al.*, 1993). It is therefore of prime interest to understand the behavior of a well-defined sample of T Tau stars.

In cool main-sequence stars, a rotation-activity relation is found for P exceeding a few days (the limit being somewhat dependent on the stellar mass or spectral type), approximately following $L_X \propto P^{-2.6}$ (Güdel *et al.*, 1997, Flaccomio *et al.*, 2003a). Given the role of the convective motion, a better independent variable may be the Rossby number $R = P/\tau$ where τ is the convective turnover time (Noyes *et al.*, 1984). If the rotation period is smaller than a few days, the X-ray luminosity saturates at a value of $L_X/L_* \approx 10^{-3}$ and stays at this level down to very short periods.

Corresponding studies of TTS have produced conflicting results. Although a relation has been indicated in TMC (Stelzer and Neuhäuser, 2001), samples in other star-forming regions show stars at saturated X-ray luminosities all the way to periods of ≈ 20 days (e.g., Preibisch *et al.* 2005a). There is speculation that these stars are still within the saturation regime because their Rossby number remains small enough for the entire range of P , given the long convective turnover times in fully convective stars.

Our nearly complete sample of TTS (for the surveyed area) permits an unbiased investigation of this question with the restriction that we know P for only 25 TTS (13 CTTS and 12 WTTS) in our sample. Another 23 stars (15 CTTS and 8 WTTS) have measured projected rotational velocities $v \sin i$ which imply upper limits to P once the stellar radius is known. In a statistical sample with random orientation of the rotation axes, the average of $\sin i$ is $\pi/4$ which we used for estimates of P if only $v \sin i$ was known. The stellar radii were calculated from T_{eff} and the (stellar) L_* .

The resulting trend is shown in Fig. 10 (the average L_X is used for stars with multiple observations; Briggs *et al.* 2006, in preparation). First, it is evident that the sample of CTTS with measured P rotates, on average, less rapidly than WTTS (characteristically, $P \approx 8$ d and 4 d, respectively). Fig. 10 shows that the rotation-activity behavior is clearly different from that of main-sequence solar-mass stars in that L_X/L_* remains at a saturation level up to longer periods. This is not entirely surprising given that the same is true for less massive main-sequence K and M-type

stars that are more representative of the TTS sample (Pizzolato *et al.*, 2003). The trend is even clearer when plotting the average X-ray surface flux, in particular for periods exceeding ≈ 5 d (Briggs *et al.*, 2006, in preparation), supporting previous ROSAT studies (Stelzer and Neuhäuser, 2001).

Why this finding is at variance from findings in Orion (Preibisch *et al.*, 2005a) is unclear. One possibility are unknown survey biases (Briggs *et al.*, 2006, in preparation). Another reason is the (on average) larger age of TMC in which a larger fraction of stars may have developed a radiative core (Briggs *et al.*, 2006, in preparation).

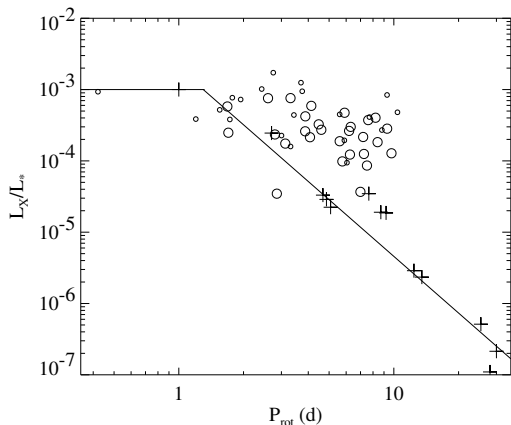


Fig. 10.— The ratio L_X/L_* as a function of rotation period for the TMC sample (Briggs *et al.*, 2006, in preparation). Symbols are as in Fig. 7. The crosses and the schematic power-law fit resp. horizontal saturation law apply to a sample of solar analogs on the main sequence (Güdel *et al.*, 1997).

6.3 Accretion and Disks

In the standard dynamo interpretation, the (on average) slower rotation of the CTTS compared to WTTS and their (on average) slightly lower L_X are well explained by a decreasing dynamo efficiency with decreasing rotation rate. This is the conventional explanation for the activity-rotation relation in aging main-sequence stars. The relation suggested above could, however, be mimicked by the CTTS sample, rotating less rapidly, being subject to suppressed X-ray production for another reason than the decreasing efficiency of the rotation-induced dynamo. We already found that the average L_X/L_* is smaller by a factor of two for CTTS compared to WTTS (Section 6.1). The most obvious distinction between CTTS and WTTS is active accretion from the disk to the star for the former class.

There are two arguments against this explanation. First, a rotation-activity relation holds *within* the CTTS sample, and there is no obvious correlation between P and the mass accretion rate, \dot{M} , for that sample. And second, when investigating the coronal properties L_X , L_X/L_* (and also average coronal temperature T_{av}) as a function of the mass accretion rate (as given by White and Ghez, 2001; Hartigan and Kenyon, 2003; White and Hillenbrand, 2004), we

see no trend over three orders of magnitude in \dot{M} (Fig. 11 for L_X ; Telleschi *et al.*, 2006, in preparation). Mass accretion rate does therefore not seem to be a sensitive parameter that determines overall X-ray coronal properties. It therefore rather seems that CTTS produce, on average, lower L_X because they are typically rotating more slowly, which may be related to disk-locked rotation enforced by star-disk magnetic fields (e.g., Montmerle *et al.*, 2000).

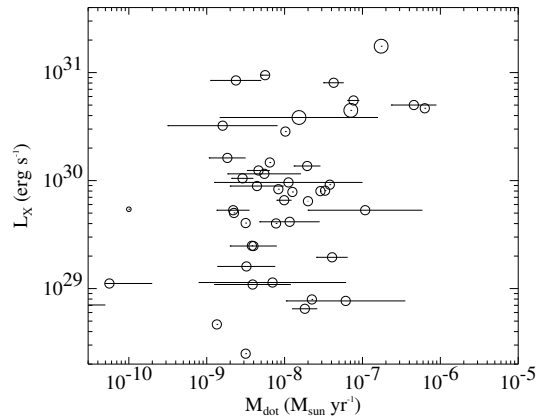


Fig. 11.— Scatter plot of L_X versus the (range of) mass accretion rates reported in the literature. No trend is evident. Symbols are as in Fig. 7. (Telleschi *et al.* 2006, in preparation.)

7. JETS AND OUTFLOWS

Shock speeds in the high-velocity component of protostellar jets may be sufficient to shock-heat plasma to X-ray temperatures. The shock temperature is $T \approx 1.5 \times 10^5 v_{100}^2$ K where v_{100} is the shock front speed relative to a target, in units of 100 km s^{-1} (Raga *et al.* 2002). Jet speeds in TMC are typically of order $v = 300 - 400 \text{ km s}^{-1}$ (Eisloffel and Mundt, 1998; Anglada, 1995; Bally *et al.*, 2003), allowing for shock speeds of similar magnitude. If a flow shocks a standing medium at 400 km s^{-1} , then $T \approx 2.4 \text{ MK}$. X-rays have been detected from the L1551 IRS-5 protostellar jet about $0.5 - 1''$ away from the protostar, while the central star is entirely absorbed by molecular gas (Bally *et al.*, 2003).

X-rays cannot be traced down to the acceleration region or the collimation region of most protostellar jets because of the considerable photoelectric absorption in particular of the very soft X-ray photons expected from shocks (energy $\lesssim 0.5 \text{ keV}$). An interesting alternative is provided by the study of strong jets and micro-jets driven by optically revealed T Tau stars. Hirth *et al.* (1997) surveyed TMC CTTS for evidence of outflows and microjets on the $1''$ scale, identifying low-velocity (tens of km s^{-1}) and high-velocity (up to hundreds of km s^{-1}) flow components in several of them.

X-ray observations of these jet-driving CTTS have revealed new X-ray spectral phenomenology in at least three, and probably four, of these objects in TMC (DG Tau A, GV Tau A, DP Tau, and tentatively CW Tau - see Fig. 12;

Güdel *et al.*, 2005; Güdel *et al.*, 2006b). They share X-ray spectra that are composed of two different emission components subject to entirely different photoelectric absorption. The soft component, subject to very low absorption ($N_{\text{H}} \approx 10^{21} \text{ cm}^{-2}$), peaks at 0.7–0.8 keV where Fe XVII produces strong emission lines, suggestive of low temperatures. This is borne out by spectral modeling, indicating temperatures of 2–5 MK. Such temperatures are not common to TTS. A much harder but strongly absorbed component (N_{H} several times 10^{22} cm^{-2}) indicates extremely hot (several tens of MK) plasma.

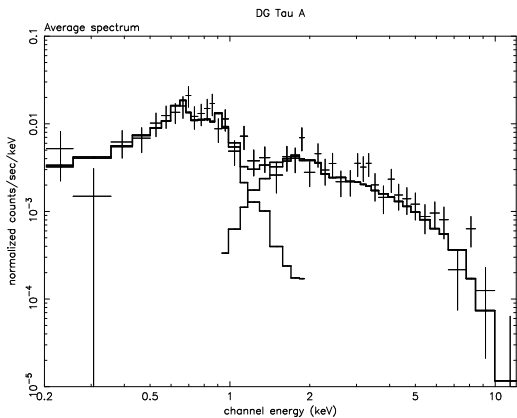


Fig. 12.— Average spectrum of DG Tau A. Also shown is the fit to the spectrum (black histogram) and its two constituents, the soft and the hard components. (Güdel *et al.*, 2006b.)

These objects show flares in their X-ray light curves (Fig. 13), but such variability is so far seen only in the hard component while the soft component is steady. Evidently, these “two-absorber” spectra require that *two physically unrelated X-ray sources are present around these objects*.

All these stars are strong accretors (\dot{M} of order 10^{-7} to $10^{-6} M_{\odot} \text{ yr}^{-1}$). However, as shown above, the TMC sample reveals no significant relation between mass accretion rate and coronal properties. The distinguishing property of these objects is, in contrast, the presence of well-developed, protostar-like jets and outflows with appreciable mass-loss rates (10^{-7} to $10^{-6} M_{\odot} \text{ yr}^{-1}$).

A tentative interpretation is the following (Güdel *et al.*, 2005; 2006b): The flaring in the hard component occurs on timescales of hours, suggesting ordinary coronal active regions. The preceding U-band bursts signal the initial chromospheric heating before plasma is evaporated into the coronal magnetic loops. The flaring active regions are therefore likely to be of modest size, well connected to the surface active regions. The excess absorption is probably due to cool gas that streams in from the disk along the magnetic field lines, enshrouding the magnetosphere with absorbing material. This increases the photoelectric absorption of X-rays but does not increase the optical extinction because the gas streams are very likely to be depleted of dust (the latter being evaporated farther away from the star). As for the cool X-ray component, although its temperature is also compatible with shock heating of material in accre-

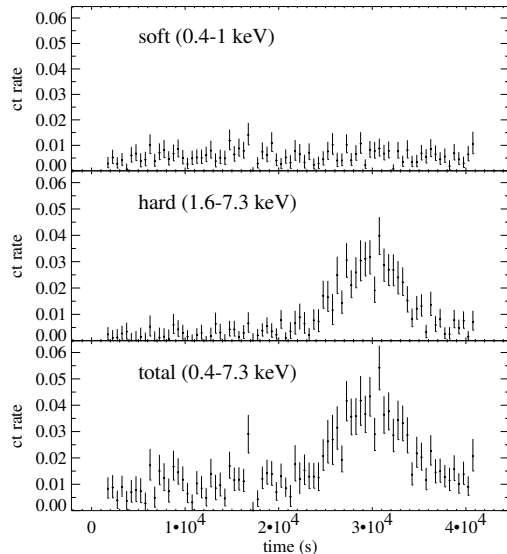


Fig. 13.— X-ray light curves of DG Tau A. The top panel shows the soft component, the middle panel the hard component, and the bottom the total X-ray light curve. (Güdel *et al.*, 2006b.)

tion columns close to the star (e.g., Kastner *et al.*, 2002), the low photoabsorption makes this interpretation problematic and prefers a location outside the magnetosphere. An obvious location of the cool, soft X-ray sources are shocks forming near the base or the collimation region of the jet (e.g., Bally *et al.* 2003). Jet speeds of several hundred km s^{-1} support this model, as do estimated X-ray luminosities (see Güdel *et al.*, 2005, based on the theory of Raga *et al.*, 2002).

If this model is correct, then the consequences are far-reaching: distributed, large-scale X-ray sources may efficiently ionize larger parts of the circumstellar environment than the central star alone, and in particular the disk surface, thus inducing disk accretion instabilities (Balbus and Hawley 1991) and altering the disk chemistry (Feigelson and Montmerle, 1999; Glassgold *et al.*, 2004).

8. SUMMARY

The Taurus Molecular Cloud provides unequalled insight into the detailed physical processes of low-mass star formation, environmental issues, astrochemistry aspects, and evolutionary scenarios down to the substellar level. New observatories now available help us tackle outstanding problems with unprecedented sensitivity, spectral and spatial resolution. Of particular interest to star-formation studies are the new X-ray observatories (*XMM-Newton* and *Chandra*), the *Spitzer* Space Telescope in the infrared, and deep, large-scale optical surveys such as the CFHT survey summarized here.

Combining the X-ray, infrared, and optical population studies, there is considerable potential for detection of new Taurus members, some of which may be strongly embedded or extinguished by their disks. Joint multi-wavelength studies have been particularly fruitful for the characterization of

brown dwarfs, which have been amply detected by all three studies and are now supporting a model in which a fraction of these objects are ejected from denser stellar aggregates.

The surveys also deepen previous studies of properties of T Tau stars and protostars (e.g., rotation-activity relations, disk properties, etc), while at the same time opening the window to new types of phenomenology such as accretion events on brown dwarfs or X-ray emission perhaps forming at the base of accelerating jets. Further insight is expected to be obtained from high-resolution (optical, IR, and X-ray) spectroscopy that should probe composition and structure of accretion disks and heated X-ray sources.

Acknowledgments. We thank our referee for constructive and helpful comments on our paper. We acknowledge extensive contributions to this work by the three TMC teams (*XMM-Newton*, *Spitzer*, and CFHT). M. Güdel specifically acknowledges help from K. Arzner, M. Audard, K. Briggs, E. Franciosini, N. Grosso (particularly also for the preparation of Fig. 1), G. Micela, F. Palla, I. Pillitteri, L. Rebull, L. Scelsi, and A. Telleschi. D. Padgett thanks J. Bouvier, T. Brooke, N. Evans, P. Harvey, J.-L. Monin, K. Stapelfeldt, and S. Strom for contributions. C. Dougados wishes to thank the whole CFHT TMC survey team, in particular F. Ménard, J. L. Monin, S. Guieu, E. Magnier, E. Martín and the CFHT astronomers (J. C. Cuillandre, T. Forveille, P. Martin, N. Manset, J. Shapiro) and director (G. Fahlman) as well as the Terapix MEGACAM data reduction center staff (Y. Mellier, G. Missonier). Research at PSI has been financially supported by the Swiss National Science Foundation (grant 20-66875.01). We thank the International Space Science Institute (ISSI) in Bern for further significant financial support to the *XMM-Newton* team. *XMM-Newton* is an ESA science mission with instruments and contributions directly funded by ESA Member States and the USA (NASA).

REFERENCES

- Adams F. C., Lada C. J., and Shu F. H. (1987) *Astrophys. J.*, 312, 788-806.
- d'Alessio P., Calvet N., Hartmann L., Lizano S., and Cantó J. (1999) *Astrophys. J.*, 527, 893-909.
- Andrews S. M. and Williams J. P. (2005) *Astrophys. J.*, 631, 1134-1160.
- Anglada G. (1995) *Rev. Mex. Astron. Astrophys.*, 1, 67-76.
- Apai D., Pascucci I., Henning Th., Sterzik M. F., Klein R., Semenov D., Günther E., and Stecklum B. (2002) *Astrophys. J.*, 573, L115-117.
- Argiroffi C., Drake J. J., Maggio A., Peres G., Sciortino S., and Harnden F. R. (2004) *Astrophys. J.*, 609, 925-934.
- Balbus S. A. and Hawley J. F. (1991) *Astrophys. J.*, 376, 214-233.
- Bally J., Feigelson E., and Reipurth B. (2003) *Astrophys. J.*, 584, 843-852.
- Barrado y Navascués D. and Martín E. (2003) *Astron. J.*, 126, 2997-3006.
- Beichman C. A., Myers P. C., Emerson J. P., Harris S., Mathieu R., Benson P. J., and Jennings R. E. (1986) *Astrophys. J.*, 307, 337-349.
- Bertin, E. and Arnouts S. (1996), *Astron. Astrophys. Suppl.*, 117, 393-404.
- Boulade O., et al. (2003) In *Instrument Design and Performance for Optical/Infrared Ground-based Telescopes* (M. Iye and A. F. M. Moorwood, eds.), pp. 72-81. The International Society for Optical Engineering.
- Bouvier J. (1990) *Astron. J.*, 99, 946-964.
- Briceño C., Hartmann L., Stauffer J., and Martín E. (1998), *Astron. J.*, 115, 2074-2091.
- Briceño C., Luhman K. L., Hartmann L., Stauffer J. R., and Kirkpatrick J. D. (2002) *Astrophys. J.*, 580, 317-335.
- Burrows A. Sudarsky D., and Lunine J. I. (2003) *Astrophys. J.*, 596, 587-596.
- Chabrier G. (2003) *Publ. Astron. Soc. Pac.*, 115, 763-795.
- Chabrier G., Baraffe I., Allard F., and Hauschildt P. (2000) *Astrophys. J.*, 542, 464-472.
- Cuillandre J., Luppino G. A., Starr B. M., and Isani S. (2000) *SPIE*, 4008, 1010-1021.
- Damiani F. and Micela G. (1995) *Astrophys. J.*, 446, 341-349.
- Damiani F., Micela G., Sciortino S., and Harnden F. R. Jr. (1995) *Astrophys. J.*, 446, 331-340.
- Dobashi K., Uehara H., Kandori R., Sakurai T., Kaiden M., Umemoto T., and Sato, F. (2005) *Publ. Astron. Soc. Japan*, 57, S1-S368.
- Duchêne G., Monin J.-L., Bouvier J., and Ménard F. (1999) *Astron. Astrophys.*, 351, 954-962.
- Durney B. R., De Young D. S., and Roxburgh, I. W. (1993) *Solar Phys.* 145, 207-225.
- Eislöffel J. and Mundt R. (1998) *Astron. J.*, 115, 1554-1575.
- Eisner J. A., Hillenbrand L. A., Carpenter J. M., and Wolf S. (2005) *Astrophys. J.*, 635, 396-421.
- Evans N. J., et al. (2003) *Publ. Astron. Soc. Pac.*, 115, 965-980.
- Feigelson E. D. and Montmerle T. (1999) *Ann. Rev. Astron. Astrophys.*, 37, 363-408.
- Feigelson E. D., Jackson J. M., Mathieu R. D., Myers P. C., and Walter F. M. (1987) *Astron. J.*, 94, 1251-1259.
- Flaccomio E., Micela G., Sciortino S., Damiani F., Favata F., Harnden F. R. Jr., and Schachter J. (2000) *Astron. Astrophys.*, 355, 651-667.
- Flaccomio E., Micela G., and Sciortino S. (2003a) *Astron. Astrophys.*, 402, 277-292.
- Flaccomio E., Damiani F., Micela G., Sciortino S., Harnden F. R. Jr., Murray S. S., and Wolk S. J. (2003b) *Astrophys. J.*, 582, 398-409.
- Fleming T. A., Giampapa M. S., Schmitt J. H. M. M., and Bookbinder J. A. (1993) *Astrophys. J.*, 410, 387-392.
- Galfalk M., et al. (2004) *Astron. Astrophys.*, 420, 945-955.
- García-Alvarez D., Drake J. J., Lin L., Kashyap V. L., and Ball B. (2005) *Astrophys. J.*, 621, 1009-1022.
- Ghez A. M., Neugebauer G., and Matthews K. (1993) *Astron. J.*, 106, 2005-2023.
- Glassgold A. E., Najita J., and Igea J. (2004) *Astrophys. J.*, 615, 972-990.
- Gómez M., Hartmann L., Kenyon S. J., and Hewett R. (1993) *Astron. J.*, 105, 1927-1937.
- Goodwin S. P., Whitworth A. P., and Ward-Thompson D. (2004) *Astron. Astrophys.*, 419, 543-547.
- Grosso N., et al. (2006a) *Astron. Astrophys.*, in press.
- Grosso N., Audard M., Bouvier J., Briggs K., and Güdel M. (2006b) *Astron. Astrophys.*, in press.
- Güdel M. (2004) *Astron. Astrophys. Rev.*, 12, 71-237.

- Güdel M. (2006a) *Astron. Astrophys.*, in press.
- Güdel M. (2006b) *Astron. Astrophys.*, in press.
- Güdel M., Guinan E. D., and Skinner S. L. (1997) *Astrophys. J.*, 483, 947-960.
- Güdel M., Skinner, S. L., Briggs, K. R., Audard, M., Arzner, K., and Telleschi, A. (2005), *Astrophys. J.*, 626, L53-56.
- Guieu S., Pinte C., Monin J.-L., Ménard F., Fukagawa M., Padgett D., Carey S., Noriega-Crespo A., and Rebull L. (2005) In *PPV Poster Proceedings*
<http://www.lpi.usra.edu/meetings/ppv2005/pdf/8096.pdf>
- Guieu S., Dougados C., Monin J.-L., Magnier E., and Martín E. L. (2006) *Astron. Astrophys.*, 446, 485-500.
- Gullbring E., Hartmann L., Briceño, C., and Calvet, N. (1998) *Astrophys. J.*, 492, 323-341
- Hartmann L. Megeath S. T., Allen L., Luhman K., Calvet N., D'Alessio P., Franco-Hernandez R., and Fazio G. (2005) *Astrophys. J.*, 629, 881-896.
- Hartigan P. and Kenyon S. J. (2003) *Astrophys. J.*, 583, 334-357.
- Hirth G. A., Mundt R., and Solf J. (1997) *Astron. Astrophys. Suppl.*, 126, 437-469.
- Jayawardhana R., Mohanty S., and Basri G. (2002) *Astrophys. J.*, 578, L141-144.
- Jayawardhana R., Mohanty S., and Basri G. (2003) *Astrophys. J.*, 592, 282-287.
- Kaifu, N., et al. (2004) *Publ. Astron. Soc. Japan*, 56, 69-173.
- Kastner J. H., Huenemoerder D. P., Schulz N. S., Canizares C. R., and Weintraub D. A. (2002) *Astrophys. J.*, 567, 434-440.
- Kenyon S. J. and Hartmann L. (1995) *Astrophys. J. Suppl.*, 101, 117-171.
- Kenyon S. J., Hartmann L. W., Strom K. M., and Strom S. E. (1990) *Astrophys. J.*, 99, 869-887.
- Kenyon S. J., Dobrzycka D., and Hartmann L. (1994) *Astron. J.*, 108, 1872-1880.
- Kroupa P. and Bouvier J. (2003) *Mon. Not. R. Astron. Soc.*, 346, 343-353.
- Kun M. (1998) *Astrophys. J. Suppl.*, 115, 59-89.
- Leinert Ch., Zinnecker H., Weitzel N., Christou J., Ridgway S. T., Jameson R., Haas M., and Lenzen R. (1993) *Astron. Astrophys.*, 278, 129-149.
- Liu M. C., Najita J., and Tokunaga A. T. (2003) *Astrophys. J.*, 585, 372-391.
- Loinard L., Mioduszewski A. J., Rodríguez L. F., González R. A., Rodríguez M. I., and Torres R. M. (2005) *Astrophys. J.*, 619, L179-L182.
- Luhman K. L. (2000) *Astrophys. J.*, 544, 1044-1055.
- Luhman K. L. (2004) *Astrophys. J.* 617, 1216-1232.
- Luhman K. L., Briceño C., Stauffer J. R., Hartmann L., Barrado Y Navascués, D., and Caldwell N. (2003) *Astrophys. J.* 590, 348-356.
- Magnier E. A. and Cuillandre J.-C. (2004) *Publ. Astron. Soc. Pac.*, 116, 449-464.
- Martín E. L., Dougados C., Magnier E., Ménard F., Magazzù A., Cuillandre J.-C., and Delfosse X., (2001) *Astrophys. J.*, 561, L195-198.
- Mathieu R. D. (1994) *Ann. Rev. Astron. Astrophys.*, 32, 465-530.
- Mohanty S., Jayawardhana R., and Basri G. (2005) *Astrophys. J.*, 626, 498-522.
- Monin J.-L., Dougados C., and Guieu S. (2005) *Astron. Nachrichten*, 326, 996-1000.
- Montmerle T., Grosso N., Tsuboi Y., and Koyama K. (2000) *Astrophys. J.*, 532, 1097-1110.
- Moraux E., Bouvier J., Stauffer J. R., and Cuillandre J.-C. (2003) *Astron. Astrophys.*, 400, 891-902.
- Muzerolle J., Luhman K. L., Briceño C., Hartmann L., and Calvet N. (2005) *Astrophys. J.*, 625, 906-912.
- Myers P. C., Fuller G. A., Mathieu R. D., Beichman C. A., Benson P. J., Schild R. E., and Emerson J. P. (1987) *Astrophys. J.*, 319, 340-357.
- Neuhäuser R., Sterzik M. F., Schmitt J. H. M. M., Wichmann R., and Krautter J. (1995) *Astron. Astrophys.*, 297, 391-417.
- Noyes R. W., Hartmann, L. W., Baliunas S. L., Duncan D. K., and Vaughan A. H. (1984) *Astrophys. J.*, 279, 763-777.
- Onishi T., Mizuno A., Kawamura A., Tachihara K., and Fukui Y. (2002), *Astrophys. J.*, 575, 950-973.
- Padgett D. L., et al. (2004) *Astrophys. J. Suppl.*, 154, 433-438.
- Papovich C., et al. (2004) *Astrophys. J. Suppl.*, 154, 70-74.
- Pizzolato N., Maggio A., Micela G., Sciortino S., and Ventura P. (2003) *Astrophys. J.*, 397, 147-157.
- Pravdo S. H., Feigelson E. D., Garmire G., Maeda Y., Tsuboi Y., and Bally J. (2001) *Nature*, 413, 708-711.
- Preibisch T. and Zinnecker H. (2001) *Astron. J.*, 122, 866-875.
- Preibisch T., et al. (2005a) *Astrophys. J. Suppl.*, 160, 401-422.
- Preibisch T., et al. (2005b) *Astrophys. J. Suppl.*, 160, 582-593.
- Raga A. C., Noriega-Crespo A., and Velázquez P. F. (2002), *Astrophys. J.*, 576, L149-152.
- Reipurth B. and Clarke C. (2001) *Astron. J.*, 122, 432-439.
- Rieke G. H., et al. (2004) *Astrophys. J. Suppl.*, 154, 25-29.
- Scelsi L., Maggio, A., Peres G., and Pallavicini R. (2005) *Astron. Astrophys.*, 432, 671-685.
- Siess L., Dufour E., and Forestini M. (2000) *Astron. Astrophys.*, 358, 593-599.
- Simon M., et al. (1995) *Astrophys. J.*, 443, 625-637.
- Slesnick C. L., Hillenbrand L. A., and Carpenter J. M. (2004), *Astrophys. J.*, 610, 1045-1063.
- Stapelfeldt K. R. and Moneti A. (1999) In *The Universe as Seen by ISO* (P. Cox and M. F. Kessler, eds.), pp. 521-524. European Space Agency.
- Stelzer B. and Neuhäuser R. (2001) *Astron. Astrophys.*, 377, 538-556.
- Strom K. M. and Strom S. E. (1994) *Astrophys. J.*, 424, 237-256.
- Strom K. M., Strom S. E., Edwards S., Cabrit S., and Skrutskie M. (1989) *Astron. J.*, 97, 1451-1470.
- Strom K. M., Strom S. E., Wilkin F. P., Carrasco L., Cruz-Gonzalez I., Recillas E., Serrano A., Seaman R. L., Stauffer J. R., Dai D., and Sottile J. (1990) *Astrophys. J.*, 362, 168-190.
- Telleschi A., Güdel M., Briggs K., Audard M., Ness J.-U., and Skinner S. L. (2005) *Astrophys. J.*, 622, 653-679.
- Walter F. M., Brown A., Mathieu R. D., Myers P. C., and Vrba F. J. (1988) *Astron. J.*, 96, 297-325.
- Weaver W. B. and Jones G. (1992) *Astrophys. J. Suppl.*, 78, 239-266.
- White R. J. and Basri, G. (2003) *Astrophys. J.*, 582, 1109-1122.
- White R. J. and Ghez A. M. (2001) *Astrophys. J.*, 556, 265-295.
- White R. J. and Hillenbrand L. A. (2004) *Astrophys. J.*, 616, 998-1032.
- Young K. E., et al. (2005) *Astrophys. J.*, 628, 283-297.